Performance Evaluation and Application of the Laser Welded Joint with Filler Wire for Al-Si Coated Press-Hardened Steels

H. Pan[1,2(✉)], K. Ding[3], Y. L. Gao[3], and T. H. Wu[1,2]

[1] State Key Laboratory of Development and Application Technology of Automotive Steels (Baosteel Group), Shanghai 201900, China
hpan@baosteel.com

[2] Automobile Steel Research Institute R&D Center, Baoshan Iron and Steel Co., Ltd., Shanghai 201900, China

[3] State Key Laboratory of Advanced Special Steel, School of Materials Science and Engineering, Shanghai University, Shanghai 200444, China

Abstract. Laser welding of Al-Si coated press-hardened steel (PHS) is considered as a challenge in its practical application due to the possible formation of bulk blocky ferrite in the weld metal (WM). In the present study, the relationship between the mechanical properties and the microstructure was investigated. The tensile test results showed that the tensile strength for the specimens ruptured in the gauge length were all over 1450 MPa accompanied with the elongation over 4%. Based on the fatigue tests, the fatigue strength by up-and-down method was around 9.2×10^3 N. The Charpy impact tests showed that the average obtained impact energy were all around 19 J for the welded joints at room temperature and decreased temperature as low as −40 °C. In particular, no obvious ferrite could be traced in the WM. In addition, the negligible microhardness fluctuation was considered as the main factor devoting to the superior comprehensive properties of the laser welded joint of Al-Si coated PHS. In this case, the automotive safety component of door ring with satisfied quality has been successfully fabricated.

Keywords: Laser welding · Press-hardened steel · Al-Si coating · Tensile strength · Fatigue

1 Introduction

Al-Si coated press-hardened steel (PHS) is widely applied in the automotive safety components such as A-pillars, B-pillars, door rings, bumpers, roof rails, and tunnels [1–3]. With the improvement of the vehicle lightweight and the safety requirements, the door rings fabricated by the laser tailor-welded PHS blanks have been gradually focused in recent years [4, 5]. The general production procedure for the PHS with the ultimate tensile strength of over 1500 MPa could be briefly introduced as follows: PHS sheets with ferritic-pearlitic microstructure were firstly laser welded. The laser tailored blank of PHS was then heated to 900–950 °C for 3–10 min and followed by the water-quenching.

Y. Zhang and M. Ma (Eds.): ICHSU 2022, AHMST 2, pp. 185–194, 2023.
https://doi.org/10.2991/978-94-6463-114-2_25

To avoid the oxidation and decarburization during the hot stamping process, coatings such as Al-Si [6], Zn [7] and Zn-Al [8, 9] etc. on the PHS are widely adopted. Among the mentioned coatings, the Al-Si coating is more widely utilized attributing to its better anticorrosion ability and high-temperature oxidation resistance [10]. Numerous studies [11–13] revealed that the mixing of the melting Al-Si coating into the molten pool and the element diffusion during laser welding and the hot stamping processes could result in the formation of the Al-rich ferrite. The microstructure of the weld metal (WM) at room temperature was therefore consisted of the lath martensite and ferrite [14]. Wang et al. [15] investigated the microstructure evolution and the properties of laser fusion zone during post-weld heat treatment on Al-Si coated press-hardened steel, and found that the WM contained δ-ferrite and α-ferrite owing to the mixing of the Al-Si coating into the WM. Sun et al. [16] detected that the α-ferrite in the WM were generally much larger than that for δ-ferrite, and the cracks were usually initiated in the region with the existence of the α-ferrite phase, forming the brittle fracture. Saha et al. [17] have identified by transmission electron microscopy (TEM) that the Al-rich second phase in the center of the WM was the non-equilibrium δ-ferrite in the as-welded condition and transformed into α-ferrite after the hot stamping. Also they deemed that the decrease of the strength and ductility of the joints in the hot-stamped condition was due to the ferrite formation in the WM rooted at the serious Al segregation [18]. Sun et al. [19] also considered that the soft α-ferrite produced in the WM could deteriorate the tensile strength of the joint.

Many efforts have been made to reduce the adverse effect of the aluminized coating and enhance the weld mechanical properties of the Al-Si-coated PHS, such as removing the coating [20], inserting interlayers [21], changing the filler [22] etc. However, these methods either required expensive equipments or reduced the production efficiency in the practical application. Without removing the Al-Si coating, the fiber laser welding of PHS sheets was applied in the present study. Meanwhile, the mechanical properties of the welded joints in the hot-stamped condition were comparatively studied. Besides, the practical application for the laser welding in the door ring is also introduced.

2 Experimental Procedure

The Al-Si coated PHS sheets with the thickness of 1.2 mm, 1.5 mm and 1.8 mm were utilized in the fabrication of the laser welded joints. The chemical composition of the PHS was listed in Table 1.

The schematic of the laser welding process was displayed in Fig. 1(a). The main laser welding parameters were listed in Table 2. After the filler-wire laser welding, the laser-welded blanks were treated with the hot stamping process, which involved the heating at 930 °C for 4 min in a resistance furnace and subsequent water-quenching to

Table 1. The chemical composition of the PHS (wt. %).

Elements	C	Si	Mn	P	S	Alt	Fe
PHS	0.23	0.24	1.18	0.011	0.002	0.05	Bal.

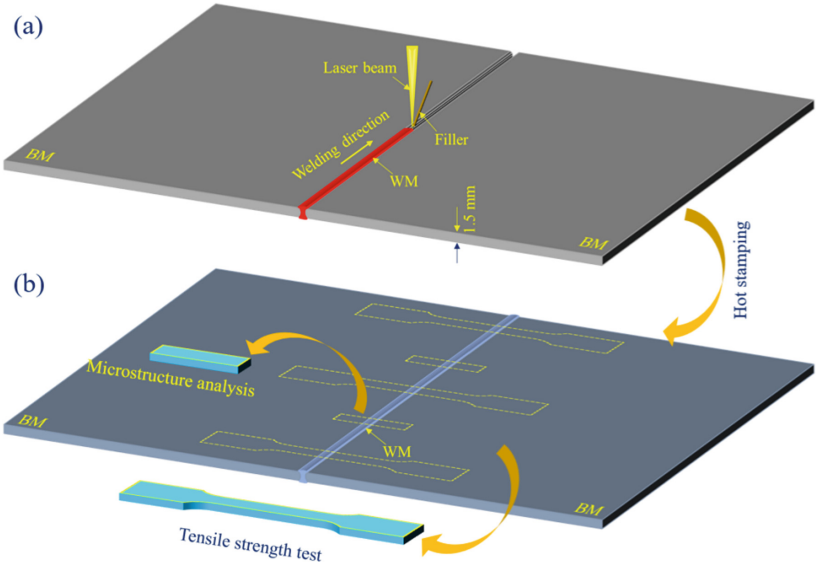

Fig. 1. Schematic of the laser welding process and sampling of the specimens for the tensile strength tests: (a) the schematic of the laser welding, and (b) the sampling schematic of the specimens.

Table 2. The main laser welding parameters employed in the experiments.

Laser power, kW	Welding speed, m/min	Filler diameter, mm	Shielding gas, L/min	Defocusing distance, mm
4.5	6	1.2	15	5

room temperature. As shown in Fig. 1(b), the cross-section specimens for microstructure observation and standard tensile specimens were cut perpendicular to weld. The microstructure was observed by optical microscopy (OM, Zeiss Image A2m) after the specimens being polished and etched by the 4% nital solution (4 mL HNO_3 + 96 mL C_2H_5OH) for 20 s. The cross tensile tests were performed on the machine of Instron 5581 with a crosshead speed of 10 mm/min. The microhardness was measured according to ASTM Standard E384. Tested by Micro Vickers (MH-5L), each microhardness point was carried out under 500 gf and 15 s holding time.

3 Results and Discussion

3.1 Tensile Strength Tests

The tensile strength tests at room temperature were carried out, and the corresponding results were displayed in Fig. 2. Figure 2(a) showed the typical appearances of the ruptured specimens. It could be found that all of the laser weld joints ruptured in the

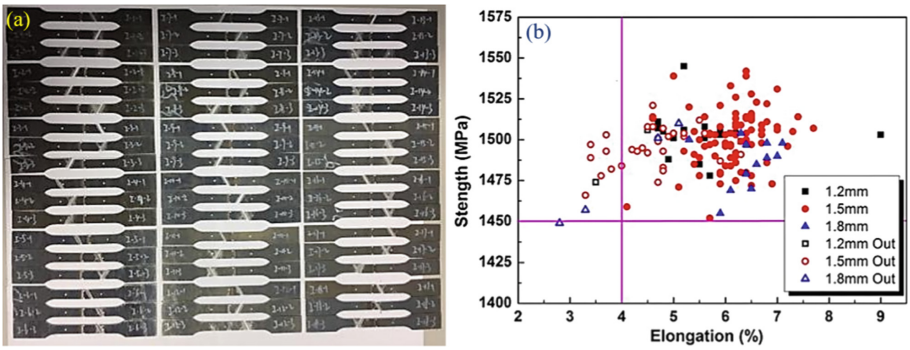

Fig. 2. The appearances and the tensile strength test results for the laser welded joints of the Al-Si coated press-hardened steel: (a) the appearances of the ruptured specimens, and (b) the tensile test results, the solid symbols represented the specimens ruptured in the gauge length, and the hollow symbols represented the specimens ruptured out the gauge length.

region away from the WM, indicating the high welding quality of the laser welded joints. In Fig. 2(b), the solid symbols represented the specimens ruptured in the gauge length, and the hollow symbols represented the specimens ruptured out the gauge length. It could be found that the tensile strength for the specimens ruptured in the gauge length were all over 1450 MPa accompanied with the elongation over 4%.

3.2 Macrostructure Observation and Microhardness Distribution

During laser welding, the Al-Si coating could be melted into the weld pool. As studied by Martin et al. [23], the increase in the Al content could stabilize the ferrite phase, which consequently caused the formation of the bulk ferrite phase along the fusion line. The main factor to induce this catastrophic failure of the laser welded Al-Si coated PHS joints was the presence of the bulk softer ferrite phase embedded in the martensitic matrix [24–26].

To shed much light on the intrinsic mechanism of the superior tensile properties for the laser welded joints, the macrostructure of the welded joint was correspondingly analyzed. Figure 3 displayed the macrostructure of the whole laser welded joints, and the boundaries of the WM could be clearly distinguished. It should be noted that no obvious ferrite phase could be detected in the WM though there existed a mixing process of the Al-Si coating into the WM, indicating the successful homogeneous mixing of the Al-Si coating in the WM by applying the optimized welding technique and parameters.

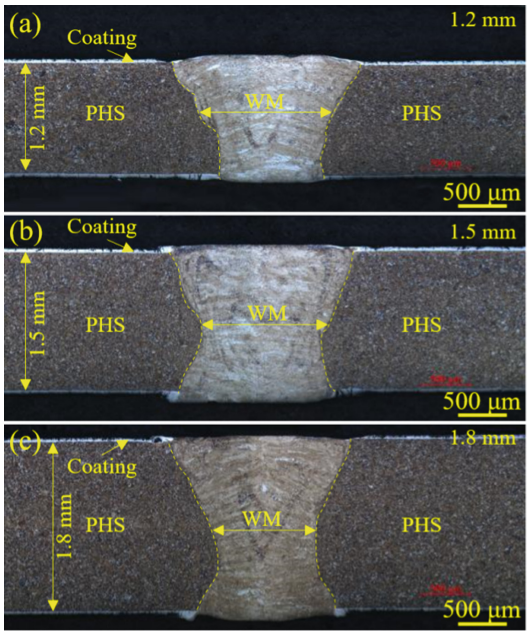

Fig. 3. The macrostructure of the laser welded joints with various thickness of steel sheets: (a) 1.2 mm, (b) 1.5 mm, and (c) 1.8 mm.

The microhardness distribution of the laser welded joints in various conditions was measured to evaluate the fluctuation. Figure 4 displayed the microhardness distribution of the laser welded joints with various thickness of steel sheets. The microhardness of the welded joints was all around 500 HV. Clearly, the microhardness fluctuation was negligible, especially for the WM.

3.3 The Assessment of the Dynamic Mechanical Properties

It is known that the superior comprehensive mechanical properties play an important role in the actual application of the laser welded joints of Al-Si coated PHS owing to the severe service conditions. The fatigue property of the welded joint is one of the important factors for reliability assessment and long-life design. Figure 5 showed the fatigue performance of the laser welded joints of Al-Si coated PHS. According to the fitting curves based on the fatigue life with various loads, it could be obtained that the fatigue strength by up-and-down load was around 9.2×10^3 N.

Furthermore, the tensile property and fatigue performance are essential, but adequate impact toughness at room temperature or even the temperatures below 0 °C should also be taken into account. The impact energies of the laser welded joints with various temperatures were obtained, and the corresponding results were listed in Table 3. It was found that the impact energies of the laser welded joints showed a high stability even tested at the temperature as low as −40 °C. The average impact energies were all around

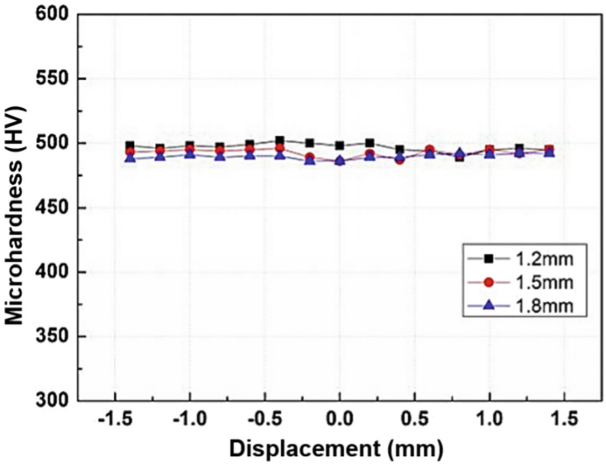

Fig. 4. Microhardness distribution of the laser welded joints with various thickness of steel sheets.

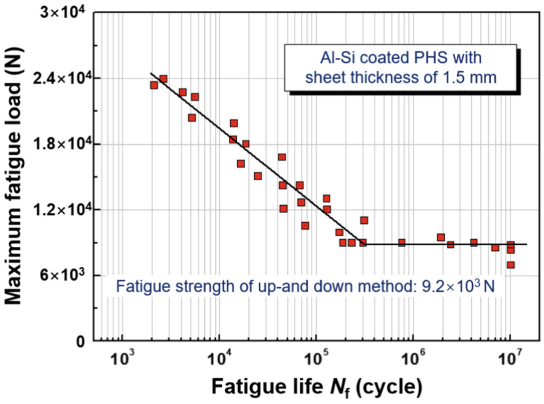

Fig. 5. The fatigue performance of the laser welded joints of Al-Si coated press-hardened steel.

19 J. In addition, the dynamic tensile tests showed that the strength of the laser welded joints could be over 1450 MPa (see Fig. 6).

Attributing to the superior comprehensive mechanical properties for the laser welded joint of the Al-Si coated PHS, the automotive safety component of door ring with satisfied quality has been successfully fabricated. The appearances of the door ring before and after the hot-stamping were displayed in Fig. 7.

Table 3. The impact energy of the laser welded joints with various temperatures.

Specimen	Temp., °C	Impact energy, J	Average impact energy, J
#1	20	19	19
#2		21	
#3		17	
#4	0	20	18.7
#5		20	
#6		16	
#7	−20	18	19
#8		18	
#9		21	
#10	−40	20	19
#11		20	
#12		17	

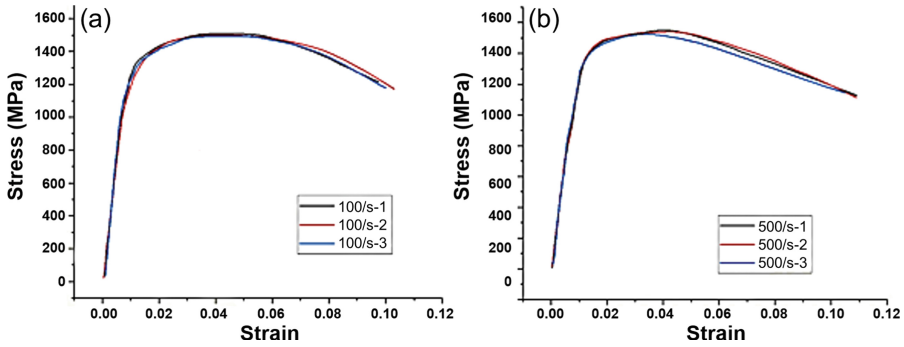

Fig. 6. The dynamic tensile tests for the laser welded joints of the Al-Si coated press-hardened steel: (a) 100/s, and (b) 500/s.

In summary, the microstructure of the WM can be controlled so that the mechanical properties of the weldment can be improved without removing the Al-Si coating prior to laser welding. The technique developed in the present study presents the feasibility of its application in automobile industry and also the anticipated potential applications in other related fields.

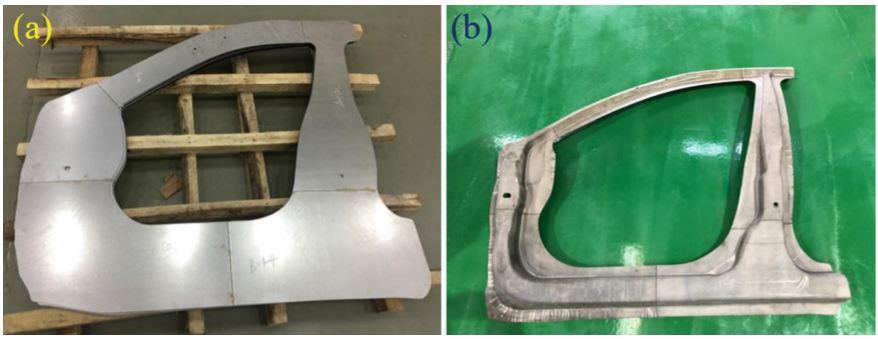

Fig. 7. The appearances of the actual components: (a) the laser welded door ring, and (b) the laser welded door ring after hot stamping.

4 Conclusions

The relationship between the mechanical properties and the microstructure was systematically investigated, the main conclusions could be summarized as follows:

1) The tensile test results showed that the tensile strength for the specimens ruptured in the gauge length were all over 1450 MPa accompanied with the elongation over 4%. Based on the fatigue tests, the fatigue strength by up-and-down load was around 9.2×10^3 N. The Charpy impact tests showed that the average obtained impact energy were all around 19 J for the welded joints at room temperature and decreased temperature as low as −40 °C.
2) The bulk ferrite could not be traced in the WM though there existed a mixing of Al-Si coating into the WM. The negligible microhardness fluctuation for the laser welded joints of Al-Si coated PHS was obtained, and the average microhardness of the welded joints was all around 500 HV.
3) The unobvious ferrite formation in the WM and the negligible microhardness fluctuation were considered as the main factors devoting to the superior comprehensive properties of the laser welded joint of Al-Si coated PHS. In this case, the automotive safety component of door ring with satisfied quality has been successfully fabricated.

References

1. M. Merklein, M. Wieland, M. Lechner, S. Bruschi and A. Ghiotti, Hot stamping of boron steel sheets with tailored properties: A review, *J. Mater. Process. Tech.* **228**, 11 (2016).
2. H. Karbasian and A. E. Tekkaya, A review on hot stamping, *J. Mater. Process. Tech.* **210**, 2103 (2010).
3. C. W. Yuan, S. C. Li, J. J. Huang, X. B. Lin, X. Z. Bian and J. M. Chen, Effect of hierarchical martensitic microstructure on fatigue crack growth behavior of ultra-high strength hot stamping steel, *Mater. Charact.* **174**, 111041 (2021).
4. L. Golem, L. Cho, J. G. Speer and K. O. Findley, Influence of austenitizing parameters on microstructure and mechanical properties of Al-Si coated press hardened steel, *Mater. Des.* **172**, 107707 (2019).

5. J. H. Moon, P. K. Seo and C. G. Kang, A study on mechanical properties of laser-welded blank of a boron sheet steel by laser ablation variable of Al-Si coating layer, *Int. J. Precis. Eng. Man.* **14**, 283 (2013).
6. Z. X. Gui, K. Wang, Y. S. Zhang and B. Zhu, Cracking and interfacial debonding of the Al–Si coating in hot stamping of pre-coated boron steel, *Appl. Surf. Sci.* **316**, 595 (2014).
7. H. Peng, W. Peng, R. Lu, G. Wu and J. Zhang, Diffusion and cracking behavior involved in hot press forming of Zn coated 22MnB5, *J. Alloys Compd.* **806**, 195 (2019).
8. J. K. Chang, C. S. Lin and W. R. Wang, Oxidation and corrosion behavior of commercial 5 wt% Al-Zn coated steel during austenitization heat treatment, *Surf. Coat. Tech.* **350**, 880 (2018).
9. J. K. Chang, C. S. Lin, W. R. Wang and S. Y. Jian, High temperature deformation behaviors of hot dip 55 wt% Al-Zn coated steel, *Appl. Surf. Sci.* **511**, 145550 (2020).
10. D. W. Fan and B. C. De Cooman, State-of-the-knowledge on coating systems for hot stamped parts, *Steel Res. Int.* **83**, 412 (2012).
11. M. Barreau, C. Methivier, T. Sturel, C. Allely, P. Drillet, S. Cremel, R. Grigorieva, B. Nabi, R. Podor, J. Lautru, V. Humblot, J. Landoulsi and X. Carrier, In situ surface imaging: High temperature environmental SEM study of the surface changes during heat treatment of an Al-Si coated boron steel, *Mater. Charact.* **163**, 110266 (2020).
12. M. H. Razmpoosh, A. Macwan, E. Biro and Y. Zhou, Effect of coating weight on fiber laser welding of Galvanneal-coated 22MnB5 press hardening steel, *Surf. Coat. Tech.* **337**, 536 (2018).
13. Y. M. Sun, L. J. Wu, C. W. Tan, W. L. Zhou, B. Chen, X. G. Song, H. Y. Zhao and J. C. Feng, Influence of Al-Si coating on microstructure and mechanical properties of fiber laser welded 22MnB5 steel, *Opt. Laser. Technol.* **116**, 117 (2019).
14. X. N. Wang, X. M. Chen, Q. Sun, H. S. Di and L. N. Sun, Formation mechanism of δ-ferrite and metallurgy reaction in molten pool during press-hardened steel laser welding, *Mater. Lett.* **206**, 143 (2017).
15. X. N. Wang, G. Yi, Q. Sun, M. Xiao, Y. Gao, Z. H. Zhang, H. S. Di and Y. N. Zhou, Study on δ-ferrite evolution and properties of laser fusion zone during post-weld heat treatment on Al-Si coated press-hardened steel, *J. Mater. Res. Technol.* **9**, 5712 (2020).
16. J. Sun, Z. Y. Han, F. Xu, X. J. Wang, H. C. Cui and F. G. Lu, The segregation control of coating element for pulse fiber laser welding of Al-Si coated 22MnB5 steel, *J. Mater. Process. Tech.* **286**, 116833 (2020).
17. D. C. Saha, E. Biro, A. P. Gerlich and N. Y. ZHou, Fusion zone microstructure evolution of fiber laser welded press-hardened steels, *Scripta Mater.* **121**, 18 (2016).
18. D. C. Saha, E. Biro, A. P. Gerlich and Y. N. Zhou, Fiber laser welding of Al-Si coated press hardened steel, *Weld. J.* **95**, 147 (2016).
19. Q. Sun, H. S. Di, X. N. Wang, X. M. Chen, X. N. Qi and J. P. Li, A study on microstructure and properties of PHS fiber laser welded joints obtained in air atmospheres, *Materials* **1135**, 1 (2018).
20. F. Li, X.G. Chen, W.H. Lin, H. Pan, X. Jin and X.M. Hua, Nanosecond laser ablation of Al-Si coating on boron steel, *Surf. Coat. Tech.* **319**, 129 (2017).
21. X. N. Wang, Z. H. Zhang, Z. R. Hu, Q. Sun, H. H. Di, F. Lv and L. N. Sun, Effect of Ni foil thickness on the microstructure of fusion zone during PHS laser welding, *Opt. Laser. Technol.* **125**, 106014 (2020).
22. W. H. Lin, F. Li, X. M. Hua and D. S. Wu, Effect of filler wire on laser welded blanks of Al-Si-coated 22MnB5 steel, *J. Mater. Process. Tech.* **259**, 195 (2018).
23. D. S. Mattin, Y. Palizdar, C. Garcia-Mateo, R. C. Cochrance, R. Brydson and A. J. Scott, Influence of aluminum alloying and heating rate on austenite formation in low carbon-manganese steels, *Metall. Mater. Trans. A* **42**, 2591 (2011).

24. C. Kim, M. J. Kang and Y. D. Park, Laser welding of Al-Si coated hot stamping steel, *Procedia Eng.* **10**, 2226 (2011).
25. D. C. Saha, E. Biro, A. P. Gerlich and Y. N. Zhou, Fiber laser welding of AlSi coated press hardened steel, *Weld. J.* **95**, 147 (2016).
26. Q. Sun, H. S. Di, X. N. Wang and X. M. Chen, Suppression of δ-ferrite formation on Al-Si coated press-hardened steel during laser welding, *Mater. Lett.* **245**, 106 (2019).